2014 IEEE International Conference on Robotics & Automation (ICRA)
Hong Kong Convention and Exhibition Center
May 31 - June 7, 2014. Hong Kong, China

A Compliant Multi-module Robot for Climbing Big Step-like Obstacles

S. Avinash, A. Srivastava, A. Purohit, S. V. Shah, K. Madhava Krishna

***Abstract*— A novel compliant robot is proposed for traversing on unstructured terrains. The robot consists of modules, each containing a link and an active wheel-pair, and neighboring modules are connected using a passive joint. This type of robots are lighter and provide high durability due to the absence of link-actuators. However, they have limited climbing ability due to tendency of tipping over while climbing big obstacles. To overcome this disadvantage, the use of compliant joints is proposed in this work. Stiffness of each compliant joint is estimated by formulating an optimization problem with an objective to minimize link joint moments while maintaining static-equilibrium. This is one of the key novelties of the proposed work. A design methodology is also proposed for developing an n-module compliant robot for climbing a given height on a known surface. The efficacy of the proposed formulation is illustrated using numerical simulations of the three and five module robots. The robot is successfully able to climb maximum heights upto three times and six times the wheel diameter using three and five modules, respectively. A working prototype was developed and the simulation results were successfully validated on it.**

I. Introduction

The aim of this paper is to propose a compliant modular robot which has enhanced step climbing ability with open-loop operation. This is one of the key functional capabilities desired in urban search and rescue(USAR) [1] and planetary exploration missions. The use of robots in such scenarios is well documented [2], [3], [4]. Specifically, urban environments predominantly consist of structured obstacles like steps, stairs, curbs, etc. A robot that can successfully navigate over these obstacles could help in creating many potential applications for robots in urban environments.

In the past, modular robots have been successfully used in USAR scenarios [5]. Unlike conventional wheeled mobile robots, the functionality of modular robots can be enhanced by adding modules [6]. Modular robots have low ground clearance and the ability to naturally deform along the obstacles on an uneven terrain. However, their ability to climb big step-like obstacles is seldom reported. This work presents a novel modular wheeled robot for climbing big-step like obstacles in an open-loop condition. The prototype of the robot is shown in Fig. 1. The proposed robot comprises of three modules, each having a link with an active wheel-pair connected to it. The adjacent modules are connected by passive joints. Such robots have been categorized in literature as Active-Wheel Passive-Joint (AW-PJ) robots [7]. Snake-like Robots such as Genbu [8] belong to this category. Several types of snake-like robots have been proposed earlier in the literature. They are broadly classified into crawler-type or wheel-type, based on the type of locomotion mechanism. They can also be classified based on the mode of actuation used for their locomotion, i.e., active-wheel/active-crawler (AW/AC) and/or active-trunk-joint (AJ). Table I depicts this classification.

*This work is not supported by any organization. All authors are with the Robotics Research Lab, IIIT-Hyderabad, India

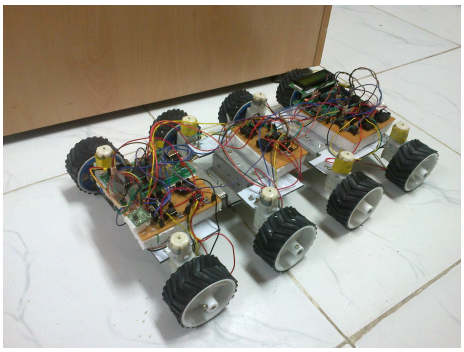

Fig. 1. A snapshot of the 3-module complaint robot prototype.

TABLE I
Classification of snake-like robots

Existing Robots	Locomotion Mechanism	Trunk Actuation	Robot Category
ACM -R4 [9]	Wheel	Active	AW-AJ
Genbu [8]	Wheel	Passive	AW-PJ
ACM-R3 [7]	Wheel	Active	PW-AJ
Shouryu III,IV,V [10], [11]	Crawler	Active	AC-AJ
Kohga [12]	Crawler	Passive	AC-PJ

While crawler robots have better climbing ability than wheeled robots, the former are slower and bulkier. Therefore, the proposed robot uses wheels for their 1) simplicity in design, 2) speed and 3) ability to provide sufficient ground clearance. It consists of three modules connected by passive link-joints and active wheels, thus belonging to the AW-PJ (active-wheel passive-link-joint) category. The use of active-link-joints for step climbing was shown in [13] using modular robot. But, robots with active-link-joints are more prone joint-motor/gear-train damage when subjected to high reaction forces/moments due to impact [14], [8]. On the other hand, snake-like robots with passive link-joints are more durable. However, they tip-over while climbing high step-like obstacles. In this work, the use of compliant joints is proposed to safeguard the robot from tipping over while climbing heights that are greater than its link length.

The use of compliant joints improves the climbing efficiency of the robot by maintaining wheel ground contact, and redistributing the normal forces for generating traction efficiently. The determination of stiffness at the compliant

joints is formulated as an optimization problem with an objective to generate minimal spring reaction moments while climbing. This is one of the main contributions of this work. Motivated by the development of this modular robot, a design methodology is also proposed for developing an n- module compliant robot for climbing a given height h on a surface whose coefficient of friction is μ. The successful validation of the methodology in developing a five module robot for climbing a step of 36 cm height is also shown.

The rest of the paper is organized as follows: Section II introduces a modular robot mechanism and analyzes the climbing behavior of passive link-joint robots. Section III presents an optimization formulation for designing compliant joints for the modular robot. In Section IV, a design methodology is proposed for developing an n-module compliant robot. The simulation results, overview of the working prototype, and its experimental validation are provided in Section V. Finally, conclusions and future work are given in Section VI.

II. Model Description

As described earlier, the proposed robot has three modules, each consisting of an independently actuated wheel-pair and a link. Neighboring modules are connected using 1 degree-of-freedom (DOF) revolute joints, called link-joints. The wheel- and link-joints are denoted by W_i and J_i, respectively, as shown in Fig. 2. The absolute (between module i and ground) and relative (between modules i and $i+1$) link joint angles are denoted by θ_i and ϕ_i, respectively.

Note that, poor module design leads to collision of links with the terrain while climbing obstacles, and resistance to the natural moment created in the favor of climbing. These two problems can be avoided by determining the minimum ground clearance and link joint placement, as discussed in [15]. The specifications of the proposed robot are listed in Table II. Before designing compliant joints, the climbing behavior of the passive modular robot is first analyzed.

Fig. 3(a) shows the climbing phase of the robot. It can be seen that module 1 will climb along the step till it crosses a limiting angle. Beyond the limiting angle the module will tip-over as shown in Fig. 3(b). The limiting angle, called tip-over angle (θ_{to}), can be determined using the center-of-mass (COM) position of the module as $\theta_{to} = \pi/2 - tan^{-1}(y_{COM}/x_{COM})$, where x_{COM} and y_{COM} denote the COM coordinates of the module. Due to tip-over, the robot can only climb obstacles of heights less than or equal to $lsin(\theta_{to})$.

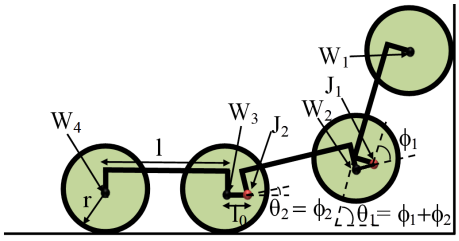

Fig. 2. The front view of the robot showing the link and wheel joints. The relative angles (ϕ's) and absolute angles (θ's) are also depicted.

TABLE II
Specifications of the 3-module robot

Symbols	Quantity	Values(with Units)
l	Link Length	0.15 m
b	Link Breadth	0.1 m
r	Wheel Radius	0.03 m
l_0	Wheel Joint and Link Joint Offset	0.03 m
τ_{wmax}	Stall Torque of Wheel Motors	0.6 Nm
m_w	Mass of Each Wheel	0.1 Kg
m_l	Mass of Each Link	0.3 Kg

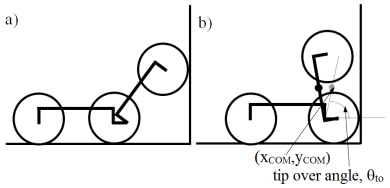

Fig. 3. Climbing behavior of the passive robot

In order to overcome this tip-over problem, we propose the use of compliant joints that are developed using torsional springs. This is one of the fundamental contributions of this work. It will be shown that the use of springs also helps in the effective redistribution of the normal forces, thus further enhancing the robot's climbing ability. These effects will be studied in sufficient detail in the next section.

III. Stiffness Estimation and Design Validation

The stiffness of a compliant joint plays a key role in the overall performance of the robot. For the robot shown in Fig. 2, designing J_1 with high stiffness causes the wheel-pair at W_2 to lift off the ground early. This results into reduction in the push force required for climbing earlier than necessary. On the other hand, applying low stiffness at J_1 might not save the module from tipping over. Therefore, an optimal value has to be estimated such that the wheel-pair lift off the ground as late as possible, and tip over is avoided. Therefore, stiffness estimation is formulated as an optimization problem with the objective to minimize moments at the joints J_1 and J_2 while climbing. Note that the dynamical effects are neglected as the robot moves with low velocities during climbing phase.

A. Optimization Formulation

Tip over can be avoided if the moments generated by springs can balance the net moment generated at the joints. For this, climbing maneuver from $h = 0$ to $2lsin\theta_{to}$ is discretized into p set points, and the moment profiles for joints J_1 and J_2 are obtained using the static stability equations. Note that, the traction and normal forces, at the wheel-ground interface, are difficult to determine accurately without direct sensing. Therefore in the numerical model, they are assumed to be unknowns and the static stability equations are under-determined [16]. Though, a least norm solution can be obtained, it may not be of physical significance. Hence, calculation of moments at the joints, and

traction and normal forces are formulated as an optimization problem. The objective function for the optimization is taken as minimization of the joint moments, as given below:

$$\underset{\mathbf{D}}{\text{minimize}} \quad \sum_{j=1}^{p} \boldsymbol{\tau}^j \qquad \text{subject to} \quad \mathbf{F} \leq \mu \mathbf{N}, \tag{1}$$

where, $\boldsymbol{\tau} = [\tau_1 \ \tau_2]^T$, $\mathbf{F} = [F_1 \ F_2 \ F_3 \ F_4]^T$, $\mathbf{N} = [N_1 \ N_2 \ N_3 \ N_4]^T$, and the vector of design variable $\mathbf{D} = [\mathbf{F}^T \ \mathbf{N}^T \ \boldsymbol{\tau}^T]^T$. Moreover, F_i's and N_i's denote traction and normal forces acting at wheel-pair i, and τ_i's denote the moments at the link joints. Note that the traction forces are constrained by the maximum torque (τ_{wmax}) of the wheel motors as $F \leq \tau_{wmax}/r$. The system is also constrained by the static stability equations of the robot, which are derived in the next subsection.

B. Quasi Static Model for the Compliant Robot

Since the robot is symmetric about the sagittal plane, a planar quasi-static analysis of the robot approximates its real behavior well. This, however, is non-trivial for the multi-module robot discussed in this paper. In mobile robots, like, CRAB [17] and PAW [16], the wheels maintain contact with the ground throughout their motion. This enables the formulation of a generalized set of equations for any arbitrary configuration. However, here, the static stability equations change when wheel-pair leaves contact with the ground during the climbing phase of the robot. Therefore, different set of equations have to considered for various configurations of the robot while optimization. In the first phase, the robot climbs heights up to $lsin\theta_{to}$ using only one link, whereas it climbs from $lsin\theta_{to}$ to $2lsin\theta_{to}$ in the next phase with two links. Figs. 4(a) and 4(b) show the two climbing phases for a 3-module robot. Equations for Phase-1 and -2 are given in (2) and (3).

$$\begin{aligned}
& & \textit{One module climbing} \\
\textstyle\sum F_x = 0 & & N_1 - F_2 - F_3 - F_4 = 0 \\
\textstyle\sum F_y = 0 & & 3w_l + 8w_w - 2F_1 - 2N_2 - 2N_3 - 2N_4 = 0 \\
\textstyle\sum M_{J_1} = 0 & & 2F_1 r + 2F_1 lcos\theta_1 + 2N_1 lsin\theta_1 - \\
& & 2w_w lcos\theta_1 - w_l[(l/2)cos\theta_1 - csin\theta_1] \\
& & - \tau_1 = 0 \\
\textstyle\sum M_{J_2} = 0 & & 2F_2 r + N_2 l - 2w_w l - w_l(l/2) - \\
& & [(2w_w + w_l) - 2F_1](l + l_0) + \tau_1 \\
& & - \tau_2 = 0 \\
\textstyle\sum M_{W_4} = 0 & & 2F_3 r + 2F_4 r + 2N_3 l - 2w_w l - w_l(l/2) - \\
& & [2(2w_w + w_l) - 2F_1 - 2N_2](l + l_0) \\
& & + \tau_2 = 0
\end{aligned} \tag{2}$$

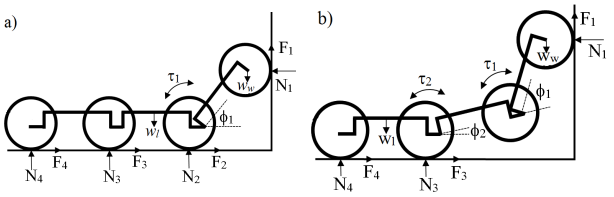

Fig. 4. Depiction of static forces and moments acting on the robot

$$\begin{aligned}
& & \textit{Two modules climbing} \\
\textstyle\sum F_x = 0 & & N_1 - F_3 - F_4 = 0 \\
\textstyle\sum F_y = 0 & & 3w_l + 8w_w - 2F_1 - 2N_3 - 2N_4 = 0 \\
\textstyle\sum M_{J_1} = 0 & & 2F_1 r + (2F_1 - 2w_w) lcos\theta_1 \\
& & - w_l[(l/2)cos\theta_1 - csin\theta_1] \\
& & + 2N_1 lsin\theta_1 - \tau_1 = 0 \\
\textstyle\sum M_{J_2} = 0 & & 2w_w(l + l_0)cos\theta_2 - w_l[(l/2)cos\theta_2 - csin\theta_2] \\
& & - [(2w_w + w_l) - 2F_1](l + l_0)cos\theta 2 \\
& & + 2N_1(l + l_0)sin\theta_2 + \tau_1 - \tau_2 = 0 \\
\textstyle\sum M_{W_4} = 0 & & 2F_3 r + 2F_4 r + 2N_3 l - 2w_w l - w_l(l/2) - \\
& & [2(2w_w + w_l) - 2F_1 - 2N_2](l + l_0) + \tau_2 = 0
\end{aligned} \tag{3}$$

where τ_{wi} is the i_{th} wheel torque, w_l and w_w are the weights of the link ($m_l g$) and wheel-pair ($m_w g$), respectively. For Phase-1, $\phi_1 = \theta_1 = sin^{-1}(h/l)$ and $\phi_2 = 0$, and for Phase-2, $\phi_2 = \theta_2 = sin^{-1}(h - lsin\theta to)/l)$ and $\phi_1 = \theta_{to} - \phi_2$. In Phase-2, ϕ_1 is designed such that if ϕ_2 increases ϕ_1 decreases by the same amount maintaining $\theta_1 = \theta_{to}$, in order to avoid tipping over.

C. Estimation of stiffness

The profile of joint moments ($\boldsymbol{\tau}$) versus joint angles ($\boldsymbol{\phi} = [\phi_1 \quad \phi_2]^T$) obtained from the above optimization is shown in Fig. 5 with a solid curve. The profile is slightly non-linear. Hence, a least squares approximation is carried out as

$$\underset{\mathbf{k}}{\text{minimize}} \quad \sum_{j=1}^{p} (\boldsymbol{\tau}^j - \mathbf{k}\boldsymbol{\phi}^j)^2 \quad , \tag{4}$$

where $\mathbf{k} = diag(k_1, k_2)$ and k is the stiffness of the i^{th} joint. The least squares fit for both the joints is also shown

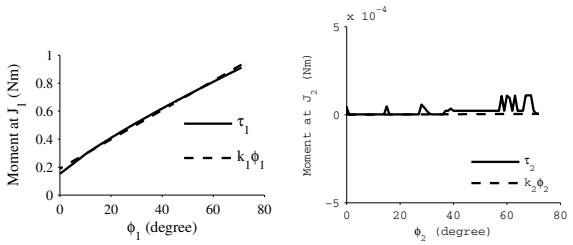

Fig. 5. Moment plots for joints J_1 and J_2: The plot shows the desired moments obtained from the optimization procedure (solid line) and the moments generated by the optimal spring (dotted line)

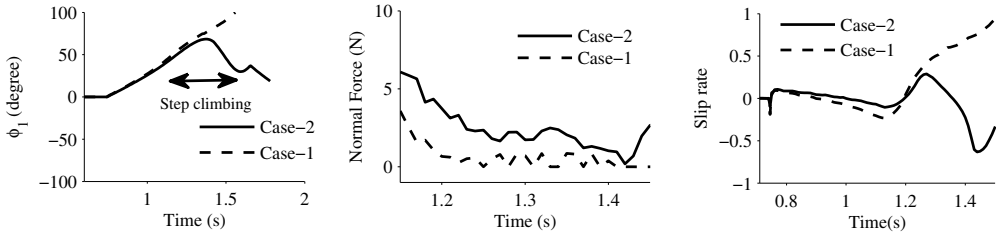

Fig. 6. Plots comparing the joint angle (ϕ_1), normal force(N_1) and slip rate(at Wheel pair-1) with spring (Case-2) and without spring (Case-1) at J_1.

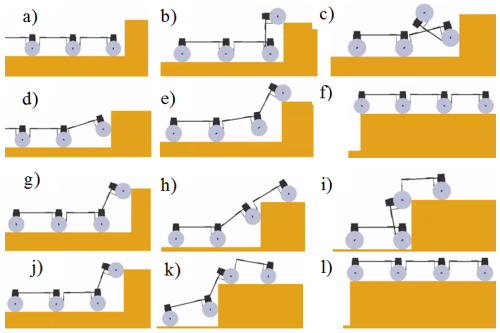

Fig. 7. Step climbing ability of the 3-module robot

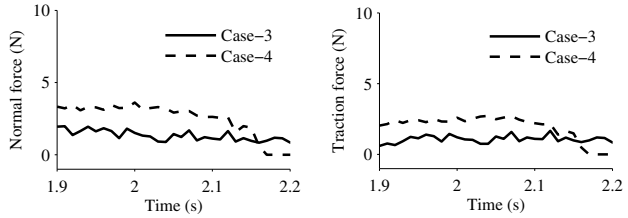

Fig. 8. Normal and Traction Force plots to study the utility of spring at J_2

in Fig. 5 by dotted lines. Values of k_1 is determined as $0.0105N - m/deg$ while k_2 is of order 10^{-6}, and hence equated to zero. According to the results obtained from the above optimization procedure, a compliant joint was developed at J_1. It is also desired that the springs only act against counter-clockwise moments and don't resist any clockwise moments. This helps in freely deforming on an uneven terrain without any resistance. Hence, the spring is fitted to module 2 and it only touches module 1 without any permanent connection. This way, the springs acts only when there is a positive angular displacement between the two modules.

D. Design Validation

Four different step climbing experiments were carried out to show the efficacy of the compliant joints in improving the climbing ability of a the robot. Each row in Fig. 7 shows the snapshots of a different experiment. In Case-1 (Fig. 7(a)-(c)), the robot consisting of joints without springs failed to climb a step of height $14\ cm$. On the other hand, the same robot (Case-2), with a spring at J_1, was able to successfully climb over, as shown in Fig. 7(d)-(f). Fig. 6(a) shows the plot of joint angles ϕ_1 for these two two cases. In Case-1, the absolute angle increased indefinitely and resulted in tip over, whereas in Case-2 the angle rose till $68^0 (\approx \theta_{to})$ and then decreased as it successfully climbed the step. The use of compliant joint in Case-2 increased the normal force, N_1, at wheel pair-1 allowing the wheels to apply more traction (F_1) and thus successfully climb without slipping, as shown in Fig. 6(b). Note that, in Case-1 wheel pair-1 lost contact with the wall multiple times, as reflected by $N_1 = 0$ in Fig. 6(b). On the other hand, in Case-2 the wheels never lost contact with the step, i.e., $N_1 > 0$. This advantage confirms the superiority of the compliant joints. Additionally, the slip rate was found to be more bounded in Case-2 than that of Case-1 as depicted in Fig. 6(c).

In Case-3 (Figs. 7(g)-(i)), the robot with a compliant joint at J_1 was made to climb a step of height $16\ cm$. Though the robot was able to climb the height, it failed to pull up the remaining modules due to the lack of push force as illustrated in Fig. 7(i). Note that the optimization only takes into consideration the climbing phase of the robot, hence, it may happen that the robot may climb height h but not have enough pulling force to lift remaining modules. In other words, the traction force F_2 reaches the limiting case μN_2 thus not allowing the wheel to apply greater traction to climb the step, as depicted in Fig. 8 with solid lines. However, this limitation can be overcome using another compliant joint at J_2 having the same stiffness value as that of J_1. In case-4 (Figs. 7(j)-(l)), the robot with two compliant joints successfully climbed a step of $16\ cm$ height. Here, the normal force at wheel-2 increased with compliance and allowed it to apply greater traction force, as shown in Fig. 8 with dotted lines. Motivated by these promising results, a generic method to developing an n-module compliant robot is conceived and detailed in the next section.

IV. Height Climbing Ability of an n-module Compliant Robot

The height climbing ability chiefly depends on the coefficient of friction μ and the maximum wheel torque τ_{wmax}. For a given modular robot design, the quasi-static analysis based optimization formulation can be used to determine the maximum climbable height, h_{max}. Next, a trajectory for tip-over-free step climbing is generated for an arbitrary large height value. It is then discretized into p set-points and the desired joint angles ϕ_i for all the set-points are estimated.

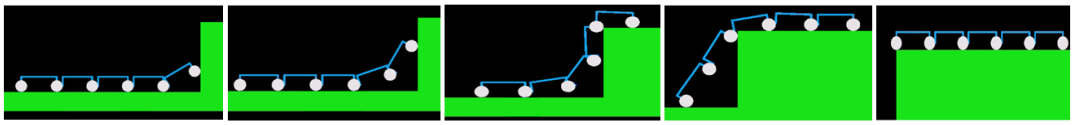

Fig. 9. A five module robot with compliant joints at J_1 and J_2 climbs a height of 36 cm

Later, they are used to obtain the static stability equations. Note that, an n-module robot has $n+1$ wheel-pairs and during the climbing maneuver, one-by-one, n wheel-pairs may lift off the ground to successfully climb without tipping over. As each wheel-pair lifts off the ground, the static-stability equations for the system change. To reflect the same, the climbing process of the robot is divided in to n phases, where each phase uses the corresponding set of static stability equations.

Phase transition occurs from Phase-i to Phase-(i+1) when $\theta_i \approx \theta_{to},\ \forall i \in n$ i.e., after every $lsin\theta_{to}$ increase in height. While evaluating the optimization procedure for all the set points, it can be noted that, at a certain set point, i.e., at a certain desired configuration of the robot, the static-stability equations are violated or a steep increase in moment values, τ_i, is noticed. The preceding set point is the height h_{max} that an n-modular robot can successfully climb. The detailed procedures for obtaining joint trajectories and static stability equations, are discussed in the following sub-sections.

A. Determination of the Joint Trajectories

$$h = \sum_{i=1}^{n} lsin\theta_i \quad where, \quad \theta_i = \sum_{i=1}^{n} \phi_i \quad \forall i \in n \tag{5}$$

$$\begin{aligned} \phi_s &= sin^{-1}(h-(s-1)lsin\theta_{to}/l) \\ \phi_{s-1} &= \theta_{to} - \phi_s \\ \phi_i &= 0 \quad \forall i \in n \backslash \{s, s-1\} \end{aligned} \tag{6}$$

$$\begin{aligned} &\textstyle\sum F_x = 0 && N_1 - \sum_{i=s+1}^{n} F_i = 0 \\ &\textstyle\sum F_y = 0 && 2(n+1)w_w + nw_l - 2F_1 - \sum_{i=s+1}^{n} N_i = 0 \\ &\textstyle\sum M_{J_1} = 0 && 2F_1 r + (2F_1 - 2w_w)lcos\theta_1 \\ & && - w_l[(l/2)cos\theta_1 - csin\theta_1] \\ & && + 2N_1 lsin\theta_1 - \tau_1 = 0 \\ &\textstyle\sum M_{J_j} = 0 && \tau_{j-1} - \tau_j - w_l[(l/2)cos\theta_j - csin\theta_j] + \\ &\forall j \in \{2, s\} && [(j-1)(w_l + 2w_w) - 2F_1)(l+l0)cos\theta_j \\ & && + 2N_1 lsin\theta_j = 0 \\ &\textstyle\sum M_{J_q} = 0 && 2F_q r + 2N_{q-1}l - 2w_w l - w_l(l/2) - \\ &\forall q \in \{n \backslash s\} && [(s+q-1)(2w_w + w_l)](l+l0) - \\ & && (2F_1 + 2\sum_{t=1}^{q-1} N_t)(l+l_0) + \tau_{q-1} - \tau_q = 0 \\ &\textstyle\sum M_{W_{n+1}} = 0 && 2F_{n+1}r + 2F_n r + 2N_{n-1}l - \\ & && [2(2w_w + w_l) - 2F_1 - 2\sum_{t=s+1}^{n} N_t](l+l_0) \\ & && - 2w_w l - w_l(l/2) + \tau_{n-1} = 0 \end{aligned} \tag{7}$$

Designing the joint trajectories for an n-module robot can be a challenging task. For this, a trajectory is developed first for the COM of the first wheel-pair and the corresponding joint motions are derived next. Trajectory of the first wheel-pair ideally follows the profile of a step or obstacle. For climbing the step, as shown in Fig. 7, trajectory of the first wheel can be assumed to be a long straight line. Next, the trajectory is discretized into p set-points and the desired joints angles (ϕ_i's) are then determined at each set-point. It is ensured that the absolute angles θ_i's of all the climbing links lie under θ_{to}, to avoid tip over. This can be achieved by progressively increasing the relative angle (ϕ_{i+1}) at the succeeding joint and decreasing that of the preceding joint (ϕ_i), as the height increases. The joint angles ϕ_i for different set-points can be obtained by solving the equations given in (5). The procedure for solving the above equations for Phases-1 and -2 have been shown in the previous section. A generalized form of the same is given in (6), to calculate the ϕ_i's for any set point in Phase-s. The joint trajectories thus obtained are used to evaluate the static stability equations of the n-module robot as shown in (7)

B. Estimation of h_{max} and $\mathbf{k}$

Section III describes in sufficient detail how the quasi-static analysis is performed for a 3-module robot. The same can be extended for an n-module robot. The final number of quasi-static equation sets is equal to the number of climbing phases s that satisfy the static-stability equations for a given robot. It can be noted that $s \in \{1, n\}$. The generalized quasi-static equations for an n-modular robot in Phase-s are given in (7). The optimization procedure is carried out for all the set points until the quasi-static constraints are violated, thus determining the maximum height, h_{max}, that the robot can climb. Thereafter, the desired moments($\boldsymbol{\tau}$) that are obtained from the optimization procedure are least squares approximated to determine the stiffness values($\mathbf{k}$) for their respective joints.

C. Illustration of Methodology

In order illustrate the proposed approach, a compliant five module robot was designed and its climbing ability was tested on surface whose μ value was 0.8. Its climbing was divided into 5 phases(as $n = 5$) and the optimization procedure was carried out for set points at increasing heights. It was noticed that the constraints were violated at a height of 50 cm, i.e., in Phase-3 of its climbing maneuver. Subsequently, the methodology was followed further, to determine the stiffness values at joints J_1 and J_2 as $k_1 = 0.024$, $k_2 = 0.029$ and $k_3 = k_4 = 0\ N-m/deg$, respectively. Figure 9 shows the snapshots of the five module robot climbing a

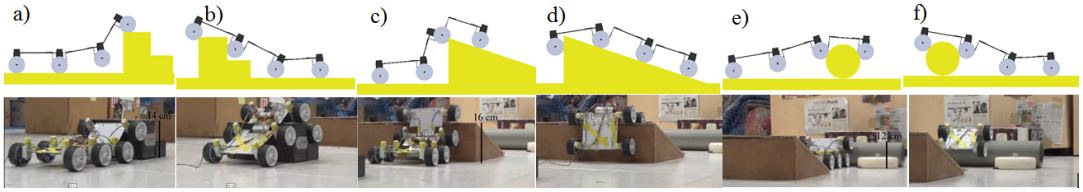

Fig. 10. Demonstrating the climbing ability of the 3-module robot in simulation (top row) and experiment (bottom row)

height of 36 cm, viz., and over two times the modules length (the module specifications are similar to those of the three module robot). In this way, the proposed methodology can be used to analyze any modular robot design.

V. Results and Discussions

Extensive simulations were carried out to demonstrate the effectiveness of compliant joints in avoiding tip over and improving the robot's step climbing ability. The results are already reported in Section-III. Figures 7, 6 and 8 show that, the use of springs has not only helped in avoiding tip-over but it also increased the normal force at the climbing wheel-pair's contact, allowing it to apply greater traction. In order to validate the simulation results, an experimental prototype of a compliant robot was developed with the same dimensions that were used in the simulation(as mentioned in Table II). Its climbing ability was assessed on different types of obstacles, first numerically, and then experimentally. Their details are presented below:

The robot was tested on an uneven terrain created using obstacles made of different materials and of varying heights, as shown in Fig. 10. The terrain consisted of a rectangular block of 14 cm height, a ramp of maximum height 16 cm and a cylindrical pipe of 12 cm diameter. The robot was able to successfully climb over all these obstacles, thus validating the effectiveness of the proposed design.

VI. Conclusions and Future Work

This work presents a methodology for designing a modular compliant robot to climb big step-like obstacles and traverse on a highly uneven terrain. The methodology is used to determine the spring stiffness values for the compliant joints by formulating an optimization problem that builds upon the quasi-static analysis of the robot. Using this methodology, three and five module robots were successfully simulated for climbing heights upto 17 cm and 36 cm, respectively. An experimental prototype of the three module robot was also built to validate the results of simulation. It is shown that the compliant joints not only helps in avoiding tip over, but also facilitate in maintaining contact between the step and the climbing wheel-pair, avoiding intermittent slip. Additionally, when a non-climbing wheel-pair leaves contact, the use of spring also helps in effective redistribution of its normal force among neighboring wheel-pairs, thereby enabling them to apply greater traction and achieve successful climbing.

The major focus of the future work would be to provide semi-autonomous capabilities to the robot. To this end, controllers will be developed for safe climbing down motion, obstacle detection, etc.

Acknowledgments

The authors would like to thank Arun Kumar Singh, Anurag VV and Priya Bansal for their support during the formative and experimental stages of this project.

References

[1] Elena Messina and Adam Jacoff. Performance standards for urban search and rescue robots. In *Defense and Security Symposium*, 2006.
[2] A. Davids. Urban search and rescue robots: from tragedy to technology. *IEEE Intelligent Systems*, 2002.
[3] Erico Guizzo. Japan earthquake: Robots help search for survivors. *IEEE Spectrum*, 2011.
[4] Erico Guizzo. Japan earthquake: More robots to the rescue. *IEEE Spectrum*, 2011.
[5] Mark Yim, Wei-Min Shen, Behnam Salemi, Daniela Rus, Mark Moll, Hod Lipson, Eric Klavins, and Gregory S Chirikjian. Modular self-reconfigurable robot systems [grand challenges of robotics]. *IEEE Robotics & Automation Magazine*, 2007.
[6] David Duff, Mark Yim, and Kimon Roufas. Evolution of polybot: A modular reconfigurable robot. In *Harmonic Drive International Symposium*, 2001.
[7] Shigeo Hirose and Hiroya Yamada. Snake-like robots [tutorial]. *IEEE Robotics & Automation Magazine*, 2009.
[8] Hitoshi Kimura and Shigeo Hirose. Development of genbu: Active wheel passive joint articulated mobile robot. In *IEEE/RSJ International Conference on Intelligent Robots and Systems (IROS)*, 2002.
[9] Hiroya Yamada and Shigeo Hirose. Development of practical 3-dimensional active cord mechanism acm-r4. *Journal of Robotics and Mechatronics*, 2006.
[10] Masayuki Arai, Toshio Takayama, and Shigeo Hirose. Development of souryu-iii: connected crawler vehicle for inspection inside narrow and winding spaces. In *IEEE/RSJ International Conference on Intelligent Robots and Systems (IROS)*, 2004.
[11] Masayuki Arai, Yoshinori Tanaka, Shigeo Hirose, Hiroyuki Kuwahara, and Shingo Tsukui. Development of souryu-iv and souryu-v: serially connected crawler vehicles for in-rubble searching operations. *Journal of Field Robotics*, 2008.
[12] Tetsushi Kamegawa, Tatsuhiro Yamasaki, Hiroki Igarashi, and Fumitoshi Matsuno. Development of the snake-like rescue robot. In *IEEE International Conference on Robotics and Automation (ICRA)*, 2004.
[13] Mark Yim, Sam Homans, and Kimon Roufas. Climbing with snake-like robots. In *IFAC Workshop on Mobile Robot Technology*, 2001.
[14] Kousuke Suzuki, Atsushi Nakano, Gen Endo, and Shigeo Hirose. Development of multi-wheeled snake-like rescue robots with active elastic trunk. In *IEEE/RSJ International Conference on Intelligent Robots and Systems (IROS)*, 2012.
[15] S Avinash, VV Anurag, AK Singh, SV Shah, and KM Krishna. A semi-active robot for steep obstacle ascent. In *IEEE International Conference on Control Applications (CCA)*, 2013.
[16] K. Turker, I. Sharf, and M. Trentini. Step negotiation with wheel traction: a strategy for a wheel-legged robot. In *IEEE International Conference on Robotics and Automation (ICRA)*, 2012.
[17] Ambroise Krebs, Thomas Thueer, Stéphane Michaud, and Roland Siegwart. Performance optimization of all-terrain robots: a 2d quasi-static tool. In *IEEE/RSJ International Conference on Intelligent Robots and Systems (IROS)*, 2006.